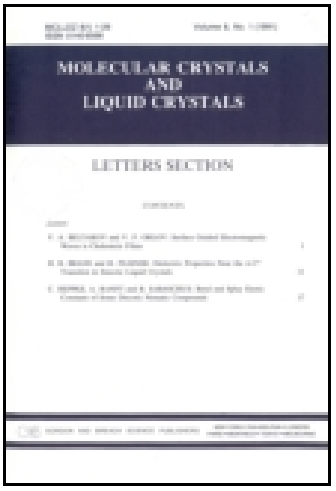

Molecular Crystals and Liquid Crystals
Publication details, including instructions for authors and subscription information:
http://www.tandfonline.com/loi/gmcl20

Enhancing Performance of Dye-Sensitized Solar Cell Utilizing by Phosphor Layer (YAG:Ce)

Young Moon Kim[a], Kyung Hwan Kim[a], Chung Wung Bark[a] & Hyung Wook Choi[a]

[a] Department of Electrical Engineering, Gachon University, 1342 SeongnamDaero, Sujeong-Gu, Seongnam-Si, Gyeonggi-Do, Republic of Korea

Published online: 06 Dec 2014.

To cite this article: Young Moon Kim, Kyung Hwan Kim, Chung Wung Bark & Hyung Wook Choi (2014) Enhancing Performance of Dye-Sensitized Solar Cell Utilizing by Phosphor Layer (YAG:Ce), Molecular Crystals and Liquid Crystals, 602:1, 88-95, DOI: 10.1080/15421406.2014.944681

To link to this article: http://dx.doi.org/10.1080/15421406.2014.944681

Mol. Cryst. Liq. Cryst., Vol. 602: pp. 88–95, 2014

ISSN: 1542-1406 print/1563-5287 online
DOI: 10.1080/15421406.2014.944681

Taylor & Francis
Taylor & Francis Group

Enhancing Performance of Dye-Sensitized Solar Cell Utilizing by Phosphor Layer (YAG:Ce)

YOUNG MOON KIM, KYUNG HWAN KIM,
CHUNG WUNG BARK, AND HYUNG WOOK CHOI*

Department of Electrical Engineering, Gachon University, Sujeong-Gu,
Seongnam-Si, Gyeonggi-Do, Republic of Korea

Generally, N-719 dye only absorbs visible light, with the wavelength ranging from 400 to 700 nm. Consequently, most of the ultraviolet (UV) radiation from the sun is not utilized by this dye. However, the UV radiation can be converted to visible light by conversion luminescence. Such visible light could then be reabsorbed by the dye in dye-sensitized solar cells (DSSCs), so that more solar irradiation could be utilized. Therefore, we used phosphors ($Y_3Al_5O_{12}:Ce^{3+}$) in DSSCs to improve the harvesting of the incident light. DSSCs coated with phosphor layers containing $Y_3Al_5O_{12}:Ce^{3+}$ showed better performance than the bare cells.

Keywords DSSC; TiO_2; phosphor; $Y_3Al_5O_{12}:Ce^{3+}$; nanoparticle; luminescence

Introduction

Since O'Regan and Graetzel first reported the highly efficient dye-sensitized solar cells (DSSCs) using nanoporous and interconnected TiO_2 particles as electrodes [1], porous thin films composed of nanosized TiO_2 particles have been widely used as electrodes in DSSCs to achieve a large surface area for the adsorption of a huge number of dye molecules, and achieve a significant increase in the photocurrent [2–13]. Generally, N-719 only absorbs visible light, having the wavelength range 400–700 nm [14]. As a result, most of the ultraviolet (UV) radiation from the sun is not utilized. In order to enhance the efficiency of DSSCs by up to 15%, both the visible light and UV radiation from the sun must be utilized. If the UV radiation could be converted into the visible light by conversion luminescence, which can then be reabsorbed by the dye in DSSCs, the amount solar irradiation utilized could be increased; this would effectively enhance the DSSC photocurrent. To improve the harvesting of the incident light, we used phosphors in DSSCs [15–17]. The efficiency of DSSCs can be enhanced by increasing the quantity of light absorbed by them. As a result, the efficiency of DSSCs coated with phosphor layers was higher than that of the bare cells.

In this paper, the efficient performance and characterization studies of DSSCs coated with phosphor layers are discussed.

*Address correspondence to Prof. Hyung Wook Choi, Department of Electrical Engineering, Gachon University, 1342 SeongnamDaero, Sujeong-Gu, SeongNam-Si, Gyeonggi-Do 461-701, Korea (ROK). E-mail: chw@gachon.ac.kr

Color versions of one or more of the figures in the article can be found online at www.tandfonline.com/gmcl.

Experimental

The phosphors were prepared by the combustion method. The starting materials for fabricating the YAG:Ce phosphors were $Y(NO_3)_3 \bullet 6H_2O$(99.9%, Aldrich), $Al(NO_3)_3 \bullet 9H_2O$ (99.997%, Aldrich), and $Ce(NO_3)_3 \bullet 6H_2O$ (99.999%, Aldrich). Urea was used as a reagent. $Y(NO_3)_3$, $Al(NO_3)_3$, and $Ce(NO_3)_3$ solutions were dissolved in deionized water. Then, the solution was stirred with a magnetic bar on a hot plate for 30 min in air. The mole ratio of all metal ions to urea was maintained at 1:1.

Then, the solution was heated to 100°C and stirred until the mixture became transparent. Next, the solution was rapidly heated to 300°C for combustion, and the solution became bright yellow.

After a few minutes, the solution underwent combustion, releasing a brown gas and eventually yielded the precursor, which was dried in air and sintered at 1000°C for 2 h in an alumina crucible in a box furnace. The solution containing phosphors was prepared by sintering the phosphor at 1000°C. The phosphor films were coated on a fluorine-doped tin oxide (FTO) conductive glass by a simple spin-coating process using the phosphor solution. The phosphor solute concentration was maintained at 6 wt%. Prior to spin coating, the bare FTO conductive glass was ultrasonically wet-cleaned using isopropyl alcohol. All the phosphor films were spin-coated onto wet-cleaned FTO conductive glasses at an optimized spinning rate of 3000 rpm for 30 s. After spin-coating the phosphor at room temperature, all FTO conductive glass samples were dried at 500°C to remove any solvent. A TiO_2 paste was coated onto the phosphor films using the doctor blade method. The cells coated with phosphor and TiO_2 were immersed in a dye (N719) solution at room temperature for 24 h. A counter electrode was prepared by spin-coating an H_2PtCl_6 solution onto an FTO conductive glass followed by heating at 450°C for 30 min. The dye-adsorbed TiO_2 electrode and Pt counter electrode were assembled into a sandwich-type cell and sealed with a 60-μm thick hot-melt sealant. An electrolyte solution was introduced into the counter electrode through a drilled hole. The hole was then sealed using a cover glass. The morphology of the prepared phosphor was investigated using field-emission scanning electron microscopy (FE-SEM, model S-4700, Hitachi). The measurements of photoluminescence (PL) over the range of 480–700 nm and photoluminescence excitation spectra (PLE) over 300–500 nm excitation range were carried out on 150 W Xe lamp (a spectrofluorometer, FP-6200, JASCO) at room temperature. The spectral resolution of both excitation and emission spectra, width of the slits, as well the measurement conditions such as scan speed were kept constant from sample to sample in measurements. Electrochemical impedance spectra (EIS) was measured using a Zahner Zennium-40071. An AC voltage with amplitude of around 50 mV was given. Impedance spectra were measured in the frequency range from 1 mHz to 1 MHz. The EIS spectra were fitted to an appropriate electrical analogue by means of the EC-Lab software (McScience). The active area of the resulting cell exposed to light was approximately 0.25 cm^2 (0.5 cm × 0.5 cm). The absorption spectra of the electrode films were measured using a UV-vis spectrometer (UV-vis 8453, Agilent). The conversion efficiency of the fabricated DSSCs was measured using an I–V solar simulator (Solar Simulator, McScience).

Results and Discussion

The phase purity of YAG was measured using X-ray powder diffraction (XRD). The XRD patterns of the $Y_3Al_5O_{12}:Ce^{3+}$ phosphor at 1000°C are shown in Fig. 1. The main peak, YAG (420), appeared at the sintering temperature 1000°C. Also, the YAG phase crystallized at

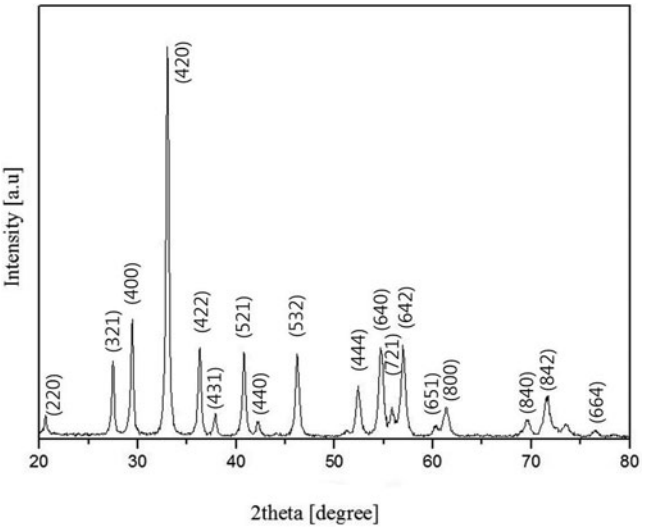

Figure 1. XRD patterns of $Y_3Al_5O_{12}:Ce^{3+}$ phosphor at 1000°C.

1000°C, which was in agreement with the Joint Committee on Powder Diffraction Standards (JCPDS) diffraction file 33–0040.

Figure 2 (a) shows the excitation spectrum of the YAG:Ce phosphor powders at 1000°C by monitoring the emission at 528 nm. The excitation bands in sample are located at 336 and 460 nm, respectively. These excitation bands are due to the electron transitions from the grand state of $Ce^{3+}(^2F_{2/5})$ to the different crystal field splitting components of excited 5*d* state of Ce^{3+} [18]. The excitation absorption band implies that ultraviolet irradiation from the sun can be absorbed by YAG:Ce. The emission spectrum of the YAG:Ce phosphor powders sintered at 1000°C is shown in Figure 2 (b). The phosphor powders show broad emission peaks over the range 500–560 nm. The emission spectrum for Ce^{3+} in sample has a maximum at 528 nm. The emission of Ce^{3+} is ascribed to the electron transitions from the lowest crystal splitting component of 5*d* level to the ground state $Ce^{3+}(^2F_{5/2}, ^2F_{7/2})$ [18].

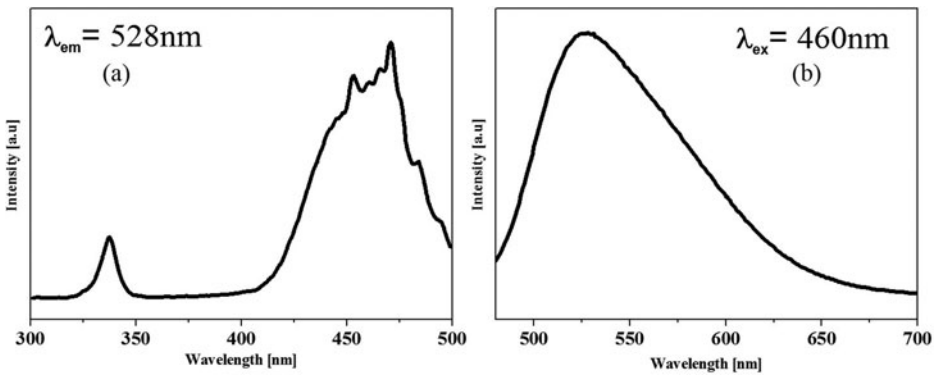

Figure 2. (a) Excitation spectrum of powder samples prepared at 1000°C; (b) emission spectrum of powder samples prepared at 1000°C.

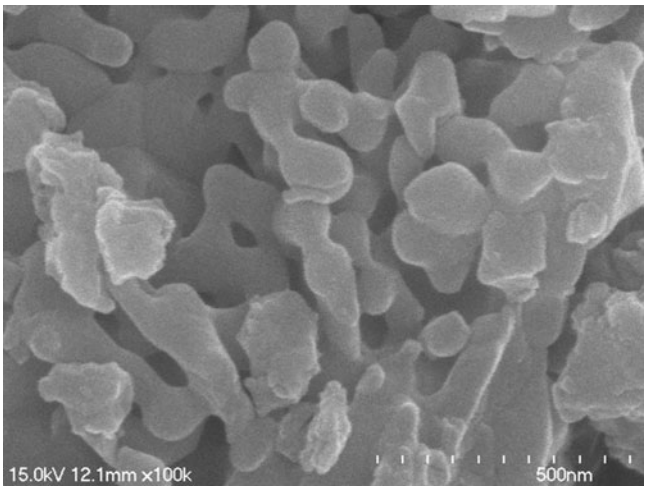

Figure 3. FE-SEM images of powder samples prepared at 1000°C.

It can be seen that YAG:Ce possess an obvious luminescence function. The luminescence around 528 nm is just within the absorption wavelength range of the sensitizing dye N-719 [14]. Combining excitation and emission spectra, the ultraviolet region of the solar irradiation can be reabsorbed by the dye N-719 via conversion luminescence by YAG:Ce. Therefore, the solar light harvest of corresponding DSSCs may be increased.

Figure 3 shows the SEM images of the YAG:Ce phosphor at 1000°C. Uniform and spherical nanoparticles of YAG:Ce phosphor with homogeneous structures were obtained by the combustion method at 1000°C. The mean size of the particles measured using the SEM image was <50 nm at 1000°C.

Figure 4 shows the electrochemical impedance spectroscopy (EIS) Nyquist plots of DSSCs with different numbers of phosphor layers at an open-circuit voltage. EIS is a

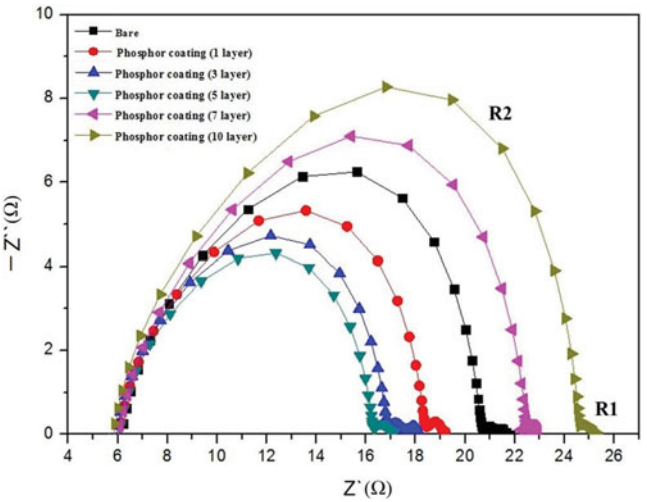

Figure 4. Nyquist plot of DSSCs with different numbers of phosphor layers at open-circuit voltage.

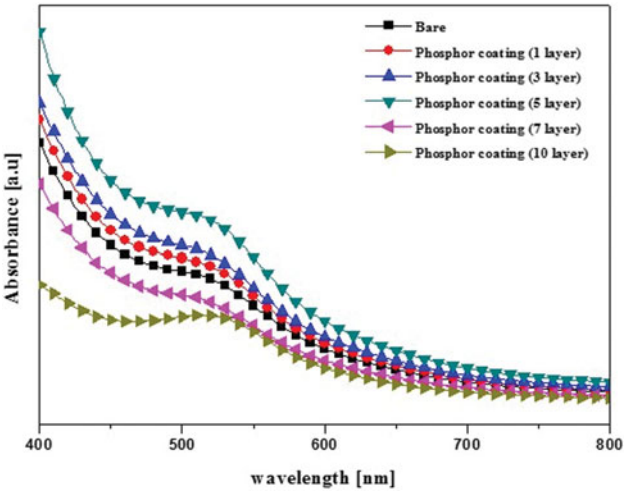

Figure 5. UV-vis absorbance of DSSCs coated with phosphor layers.

useful method for the analysis of charge-transport processes and internal resistances [19]. EIS analysis was conducted to examine the electron-transport and recombination in the DSSCs. The small semicircle in the figure is fitted to a charge-transfer resistance (R_{CT1}) and a constant phase, and the large semicircle is fitted to a transport resistance (R_{CT2}) and a constant phase [20]. The R_{CT2} circle is minimum for the DSSCs coated with five layers of phosphor, which is related to the charge-transfer resistances of FTO/TiO_2 and TiO_2/electrolyte interfaces. However, R_{CT2} values increased with increasing over 7 times. The enlargement of R_{CT2} means an increase of the recombination rate and indicates slow electron-transfer processes in the DSSCs. The reason is that with the increase of the YAG:Ce content in TiO_2, crystal defects are produced that cause a higher electron transport resistance [21]. The inefficient charge-transfer paths increase the recombination rate of electrons with I^{3-} or the oxidizing dye, resulting in a low photocurrent density and conversion efficiency [22].

Figure 5 shows the UV-vis absorbance of DSSCs coated with phosphor layers. The sample coated with 5 time showed the highest absorbance over the wavelength range 400–800 nm. Obviously, this is due to the conversion luminescence of phosphor from reabsorption by dye in the DSSC. The increase comes from results in that more incident light being harvested, thus increasing J_{sc} [23]. Manuscript in Table 1, increases J_{sc} with the

Table 1. J_{sc}, V_{oc}, FF, and efficiency

Sample	J_{sc} (mA/cm^2)	V_{oc} (V)	FF (%)	Efficiency (η)
Bare cell	10.37	0.644	73.50	4.91
Phosphor coating (1 layer)	12.12	0.658	63.35	5.05
Phosphor coating (3 layers)	13.25	0.659	62.02	5.41
Phosphor coating (5 layers)	13.89	0.682	64.12	6.08
Phosphor coating (7 layers)	9.49	0.706	68.06	4.56
Phosphor coating (10 layers)	7.41	0.726	73.81	3.97

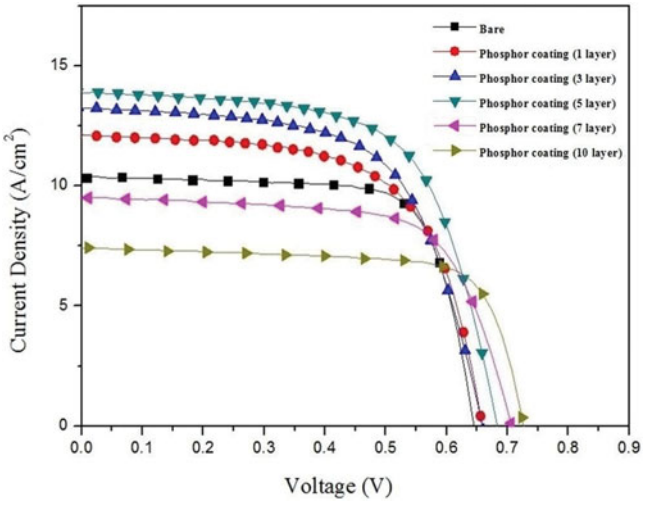

Figure 6. Photovoltaic parameters of DSSCs.

thick of phosphor increase until the phosphor layer (5 times), beyond which, J_{sc} decreases. The decrease of J_{sc} is due to the fact that introduction of rare-earth oxides produces defects in the oxide film, which causes the recombination of photoinduced holes and electrons and the decrease of J_{sc} [21].

Figure 6 shows the I–V photovoltaic performance curves of DSSCs, with and without a coating of a phosphor layer, under air mass (AM) 1.5 illumination (100 mW cm^{-2}). The equivalent values based on the duration of coating for the phosphor layers are summarized in Table 1. The efficiency of DSSCs coated with the phosphor layers was 6.08%, which was higher than that of the bare cell. DSSCs coated with five phosphor layers showed the highest efficiency at 6.08%, with J_{sc} = 13.89 mA/cm^2, V_{oc} = 0.682 V, and FF = 64.12%. However, the efficiency decreased when more than seven layers of the phosphor were coated on to DSSCs, because the increased thickness of the resulting phosphor layer increased the impedance. The value of V_{oc} increased on increasing the number of phosphor layers. Moreover, compared to the standard, the value of V_{oc} of the coated electrodes slightly improved (see Table 1). V_{oc} increases on increasing percentage of YAG:Ce. V_{oc} of the DSSCs depends on the energy level of the electrons in the oxide film and the redox potential of the electrolyte [14, 24]. If Ce^{3+} ions substitute Ti^{4+} ions at the Ti-lattice sites in TiO_2, the electronic energy level of the oxide film is elevated, which leads to an increase of V_{oc} [25–26]. DSSCs coated with phosphor layers exhibited a slightly higher photocurrent density than the bare cells. Because the UV radiation could be converted into the visible light by conversion luminescence, and later reabsorbed by the dye in DSSCs, the photocurrent was effectively enhanced.

Therefore, DSSCs coated with phosphor layers containing $Y_3Al_5O_{12}:Ce^{3+}$ showed better performance than the bare cells. As a result, a coating with five phosphor layers was the optimum condition for achieving the maximum conversion efficiency.

Conclusions

The photovoltaic performances of DSSCs coated with phosphor layers (1–10 layers) were compared. The UV radiation was converted into the visible light by conversion

luminescence, and later reabsorbed by the dye in DSSCs so that more solar radiation could be utilized. As a result, the photocurrent of DSSCs was effectively enhanced. When the number of phosphor layers coated onto DSSCs was five, the efficiency of light-to-electricity conversion of the DSSCs reached 6.24% with the simulated solar radiation of 100 mW cm^{-2}. The efficiency of DSSCs coated with phosphor layers was enhanced by a factor of 1.54 compared to those without the coating. Thus, the efficiency of DSSCs coated with phosphor layers was effectively enhanced by increasing the amount of light absorbed by DSSCs.

Funding

This work was supported by the Human Resources Development program (No. 20124030200010) of the Korea Institute of Energy Technology Evaluation and Planning (KETEP) grant funded by the Korea government Ministry of Trade, Industry and Energy. This work was supported by the National Research Foundation of Korea (NRF) Grant Funded by the Korean Government (MEST) (No. 2012R1A1A2044472).

References

[1] O'Regan, B., & Gratzel, M. (1991). *Nature 353*, 737–740.
[2] Gratzel, M. (2005). *Inorg. Chem. 44*, 6841–6851.
[3] Chiba, Y., Islam, A., Komiya, R., Koide, N., & Han, L. (2006). *Appl. Phys. Lett. 88*, 223505.
[4] Kao, M. C., Chen, H. Z., Young, S. L., Kung, C. Y., & Lin, C. C. (2009). *Thin Solid Films 517*, 5096.
[5] Kim, Y. J., Lee, M. H., Kim, H. J., Lim, G., Choi, Y. S., Park, N. G., Kim, K., & Lee, W. I. (2009). *Adv. Mater. 21*, 1.
[6] Mende, L. S., & Gratzel, M. (2006). *Thin Solid Films 500*, 296.
[7] Huang, C. Y., Hsu, Y. C., Chen, J. G., Suryanarayanan, V., Lee, K. M., & Ho, K. C. (2006). *Sol. Energy Mater. Sol. Cells 90*, 2391.
[8] Lee, J. K., Jeong, B. H., Jang, S. I., Yeo, Y. S., Park, S. H., Kim, J. U., Kim, Y. G., Jang, Y. W., & Kim, M. R. (2009). *J. Mater. Sci.: Mater. Electron. 20*, S446.
[9] Wu, J., Hao, S., Lin, J., Huang, M., Huang, Y., Lan, Z., & Li, P. (2008) *Cryst. Growth Des. 8*, 247.
[10] Park, N. G., Schlichthorl, G., Van de Lagrmatt, J., Cheong, H. M., Mascarenhas, A., & Frank, A. J. (1999) *J. Phys. Chem. B 103*, 3308.
[11] Hou, K., Tian, B., Li, F., Bian, Z., Zhao, D., & Huang, C. (2005). *J. Mater. Chem. 15*, 2414.
[12] Wei, M., Konishi, Y., Zhou, H., Yanagida, M., Sugihara, H., & Arakawa, H. (2006). *J. Mater. Chem. 16*, 1287.
[13] Chen, D., Huang, F., Cheng, Y., & Caruso, R. A. (2009). *Adv. Mater. 21*, 1.
[14] Gratzel, M. (2001). *Nature 414*, 338.
[15] Oelhafen, P., & Schuler, A. (2005). *Solar Energy 79*, 110–121
[16] Yang, Guangtao, Zhang, Jing, Wang, Peiqing, Sun, Qiang, Zheng, Jun, & Zhu, Yuejin (2011). *Current Applied Physics*, *11*, 376–381.
[17] Wang, Yuanzhe, Chen, Enlong, Lai, Hongmei, Lu, Bin, Hu, Zhijuan, Qin, Xiaomei, Shi, Wangzhou, & Du, Guoping (2013). *Ceramics International*, *39*, 5407–5413.
[18] Lin, J., & Su, Q. (1995). *J. Mater. Chem.*, *5*, 1151
[19] Yang, C. C., Zhang, H. Q., & Zheng, Y. R. (2011). *Current Applied Physics Supplement*, *11*, S147–S153.
[20] Xia, J. B., Masaki, N., Jiang, K. J., & Yanagida, S. (2007). *Journal of Physical Chemistry C*, *111*, 92.
[21] Murakoshi, K., Kano, G., Wada, Y., Yanagida, S., Miyazaki, H., Matsumoto, M., & Murasawa, S. (1995). *J. Electroanal. Chem.*, *396*, 27.

[22] Zhong, Min, Shi, Jingying, Zhang, Wenhua, Han, Hongxian, & Li, Can (2011). *Materials Science and Engineering B*, *176*, 1115–1122
[23] Chou, C. S., Guo, M. G., Liu, K. H., & Chen, Y. S. (2012). *Applied Energy*, *92*, 224–233
[24] Shen, H., Li, X., Li, J., Wang, W., & Lin, H. (2013). *Electrochimica Acta*, *97*, 160–166
[25] Ko, K., Lee, Y., & Jung, Y. (2005). *J. Colloid Interface Sci.*, *283*, 482
[26] Liau, L., & Lin, C. (2008). *Thin Solid Films*, *516*, 1998